

**Supplemental Information for  
Targeting iron metabolism in high grade glioma with <sup>68</sup>Ga-citrate PET/MR**

Spencer C. Behr<sup>1\*</sup>, Javier E. Villanueva-Meyer<sup>1\*</sup>, Yan Li<sup>1</sup>, Yung-Hua Wang<sup>1</sup>, Junnian Wei<sup>1</sup>, Anna Moroz<sup>1,2</sup>, Julia K.L. Lee<sup>1</sup>, Jeffrey C. Hsiao<sup>1</sup>, Kenneth T. Gao<sup>1</sup>, Wendy Ma<sup>1</sup>, Soonmee Cha<sup>1</sup>, David M. Wilson<sup>1</sup>, Youngho Seo<sup>1</sup>, Sarah J. Nelson<sup>1,3,4</sup>, Susan M. Chang<sup>3,5,†</sup>, Michael J. Evans<sup>1,3,6,†</sup>

<sup>1</sup>Department of Radiology and Biomedical Imaging, University of California San Francisco, 505 Parnassus Ave, San Francisco CA 94143

<sup>2</sup>Skolkovo Institute of Science and Technology, Skolkovo Innovation Center, 3 Nobel Street, Moscow 143026, Russia

<sup>3</sup>Helen Diller Family Comprehensive Cancer Center, <sup>4</sup>Department of Bioengineering and Therapeutic Sciences, <sup>5</sup>Department of Neurological Surgery, and <sup>6</sup>Department of Pharmaceutical Chemistry, University of California San Francisco, 505 Parnassus Ave, San Francisco CA 94143

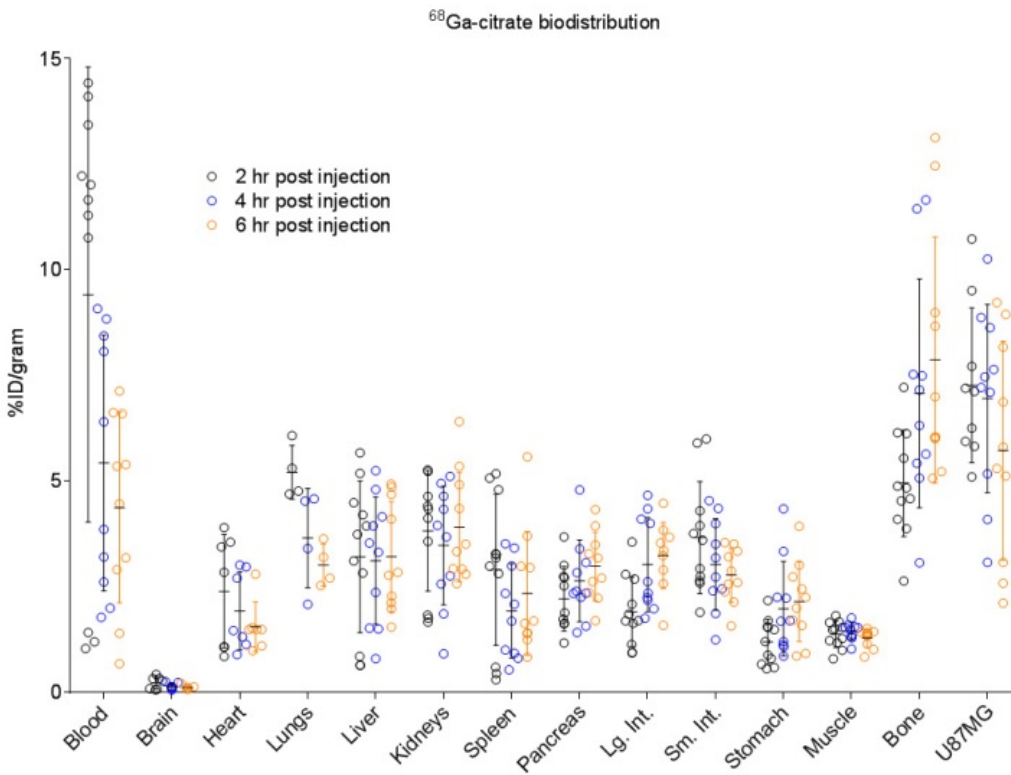
\* These authors contributed equally to this work.

† To whom correspondence should be addressed:

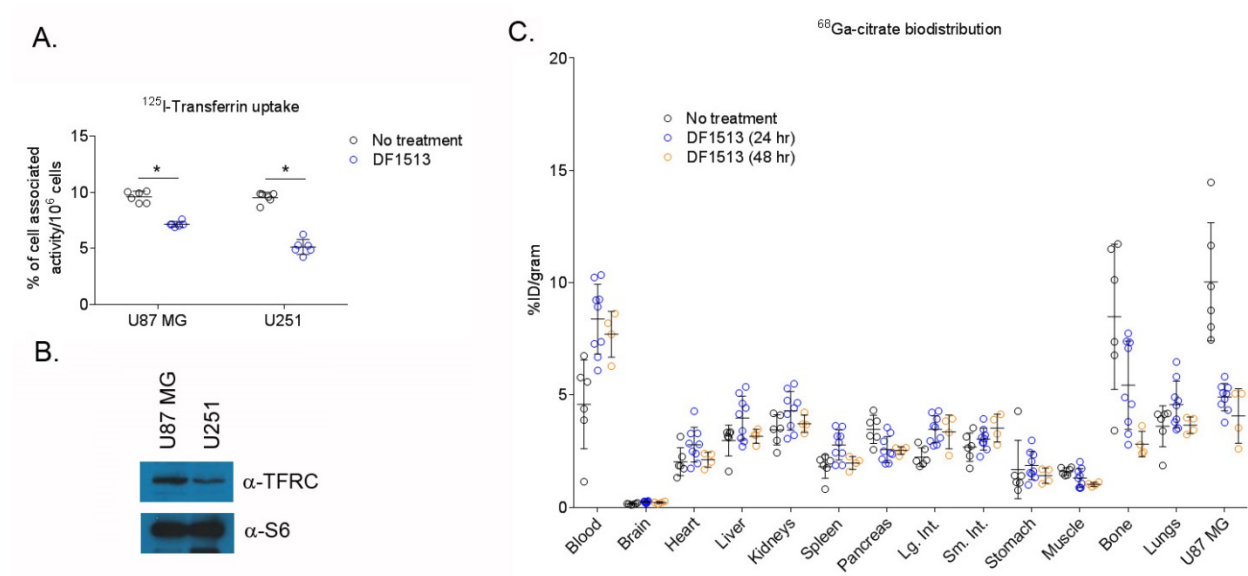
Susan M. Chang, MD  
400 Parnassus Ave  
San Francisco, CA 94143  
susan.chang@ucsf.edu

Michael J. Evans, PhD  
600 16<sup>th</sup> Street, N572C  
San Francisco, CA 94158  
michael.evans@ucsf.edu

**Supplemental Figure 1.** Biodistribution data shows the relative tissue uptake of  $^{68}\text{Ga}$ -citrate over time in intact male *nu/nu* mice bearing subcutaneous U87 MG tumors. The data represents the mean  $\pm$  standard deviation of  $n = 5$  mice/time point. The data was reproduced over two independent experiments, and the cumulative biodistribution data from both studies is presented.



**Supplemental Figure 2. A.** In vitro cellular assays shows that treatment of two human glioma cell lines with 20  $\mu\text{g}$  of DF1513 blocks the binding and uptake of  $^{125}\text{I}$ -labeled human holo transferrin. \* $P < 0.01$ , determined using an unpaired, two tailed Student's t test. The data is representative of two independent experiments. **B.** Immunoblots showing the expression of TFRC in whole cell lysates of U87 MG and U251 cells. **C.** Biodistribution data shows the relative tissue uptake of  $^{68}\text{Ga}$ -citrate 4 hours post injection in intact male *nu/nu* mice bearing subcutaneous U87 MG tumors. The data represents the mean  $\pm$  standard deviation of  $n = 5$  mice/time point. The data were reproduced with two independent experiments, and the cumulative biodistribution data is represented. Treatment arms with fewer than 10 data points are due to animal dropout from an unexpected adverse event. Mice received no treatment (no Tx), or 100  $\mu\text{g}$  of DF1513 via tail vein 24 or 48 hours prior to the administration of  $\sim 400 \mu\text{Ci}$  of  $^{68}\text{Ga}$ -citrate. Statistically significant changes between treatment arms were calculated using an unpaired, two tailed Student's t test, and the statistics are reported in text.



**Supplemental Table 1.** A summary of the patient characteristics and the imaging conditions.

See companion excel spreadsheet, titled “Behr et al\_Supplemental Table 1.xlsx”

**Supplemental Table 2.** A comparison of multiple uptake times for five patients showing increasing tumor to blood pool and tumor to white matter with longer uptake times post injection. Little improvement in signal to noise was noted after 3.5 hours post injection. The three PET acquisitions were 30 minutes apart.

<sup>68</sup> Ga-citrate dose (mCi)	Uptake time to 1 <sup>st</sup> PET (min)	# of PET avid lesions	Lesion #	Tumor:White Matter			Tumor:Blood Pool		
				1 <sup>st</sup> PET	2 <sup>nd</sup> PET	3 <sup>rd</sup> PET	1 <sup>st</sup> PET	2 <sup>nd</sup> PET	3 <sup>rd</sup> PET
5.6	102	2	1	230	240	307	0.86	1.03	1.50
			2	183	201	249	0.68	0.87	1.22
5.8	157	2	1	240	215	225	1.33	1.72	2.25
			2	90	95	75	0.5	0.76	0.75
5.6	187	1	1	199	97.5	100.5	0.55	0.65	0.67
4.4	252	2	1	358	270	344.55	1.44	1.42	1.44
			2	279	308.46	338.18	1.13	1.62	1.41
10	276	2	1	86.67	88.33	81.67	3.66	4.08	4.08
			2	62	53.33	60	2.62	2.46	3

**Supplemental Table 3.** A summary of the average  $SUV_{\text{mean}}$  values in selected normal tissues and compartments for the fourteen subjects in this study. The values presented are mean  $\pm$  standard deviation.

Normal Organ	$SUV_{\text{mean}}$
White Matter	$0.02 \pm 0.02$
Venous Blood Pool	$2.55 \pm 0.5$
Masseter Muscles	$1.06 \pm 0.2$
Parotid	$2.91 \pm 0.9$

**Supplemental Table 4.** A summary and comparison of the WHO 3 and WHO 4 lesion dimensions and PET avidity. The data are represented as mean  $\pm$  standard deviation for each quantitative dimension, and the values in parenthesis represent ranges.

WHO Grade	PET Avid Lesions (#)	MR size in cm	SUV <sub>max</sub>	SUV <sub>peak</sub>
3	11	1.68 $\pm$ 0.05 (0.5 – 3.4)	1.21 $\pm$ 0.4 (0.3-2.7)	0.80 $\pm$ 0.5 (0.0 – 2.2)
4	18	2.24 $\pm$ 1.0 (0.7-4.5)	2.25 $\pm$ 1.0 (0.3 – 3.7)	1.20 $\pm$ 0.6 (0.2 – 2.3)

**Supplemental Table 5.** A summary of the average change in  $SUV_{mean}$  for selected normal structures among the five patients that were imaged with  $^{68}Ga$ -citrate PET/MR twice.

Normal Structure	Average Change in $SUV_{mean}$
White Matter	0.002
Venous Blood Pool	-0.13
Right Masseter Muscle	0.15
Parotid	0.13